

# Deconfinement, naturalness and the nuclear-quark equation of state

Amir H. Rezaeian<sup>1,\*</sup>

<sup>1</sup>*Institute for Theoretical Physics, University of Heidelberg,  
Philosophenweg 19, D-69120 Heidelberg, Germany*

(Dated: July 4, 2018)

Baryon-loops vacuum contribution in renormalized models like the Linear sigma model and the Walecka model give rise to large unnatural interaction coefficients, indicating that the quantum vacuum is not adequately described by long-range degrees of freedom. We extend such models into nonrenormalizable class by introducing an ultraviolet cutoff into the model definition and treat the Dirac-sea explicitly. In this way, one can avoid unnaturalness. We calculate the equation of state for symmetric nuclear matter at zero temperature in a modified  $\sigma - \omega$  model. We show that the strong attraction originating from the Dirac-sea softens the nuclear matter equation of state and generates a vacuum with dynamically broken symmetry. In this model the vector-meson is important for the description of normal nuclear matter, but it obstructs the chiral phase transition. We investigate the chiral phase transition in this model by incorporating deconfinement at high density. A first-order quark deconfinement is simulated by changing the active degrees of freedom from nucleons to quarks at high density. We show that the chiral phase transition is first-order when quark decouples from the vector-meson and coincides with the deconfinement critical density.

PACS numbers: 12.39.Ki, 21.65.+f, 24.85.+p, 12.38.Lg

Keywords: Linear sigma model, nuclear and quark matter, naturalness, deconfinement

## I. INTRODUCTION

The equation of state for strongly interacting matter at finite density is needed for understanding of neutron stars [1] and heavy ion collision phenomenology [2]. One of the most interesting open questions for such system is the identification of the appropriate degrees of freedom to describe the different phases of matter. One expects that effective degrees of freedom change from baryons at low density to quarks and gluons at high density. Therefore, at high density nuclear matter undergoes a phase transition to deconfined quarks and gluons and chiral symmetry is restored. Our current knowledge about this transition is still very rudimentary since QCD lattice computation

---

\*Electronic address: Rezaeian@tphys.uni-heidelberg.de

cannot yet be performed at large density. In this paper we attempt to describe the first order liquid-gas phase transition of nuclear matter, the chiral phase transition, and the transition to quark matter in a unified framework. For this purpose, we work within an effective chiral linear sigma model coupled to nucleons and quarks.

The chiral linear sigma model and its extension have been successful in explaining the low energy physics of mesons and nucleons in vacuum due to utilizing the concept of spontaneous chiral symmetry breaking. However this model has been less successful at finite density. Very early studies by Kerman and Miller [3] showed that the linear sigma model ( $L\sigma N$ ) model with nucleonic degrees of freedom in fact does not lead to saturating nuclear matter in mean field approximation. This failure is due to the fact that in chiral models with Mexican hat potential, the medium effect moves the vacuum effective potential towards smaller values. This implies a smaller curvature and consequently the mass of the scalar field decreases. The scalar field in the linear sigma model plays the role of the chiral partner of the pion and the mediator of medium-range nucleon-nucleon attraction. Therefore, as its mass becomes smaller the attraction between nucleons becomes stronger. This simple effect may destroy the stability of nuclear matter<sup>1</sup>.

Boguta [8] showed, however, that a saturating normal ground state in the  $L\sigma N$  model can be reproduced by introducing a vector-scalar coupling in a chirally invariant way and generating a mass to the vector-meson via spontaneous symmetry breaking. In this approach the saturation stems from the cancellation of large repulsive vector mesons and attractive scalar mesons which is generated through spontaneous symmetry breaking. However, unacceptably large compression modulus of nuclear matter (about  $K \simeq 650$  MeV) still remain difficult to overcome within this approach. Another short-coming of this approach is the absence of the chiral phase transition, since the effective nucleon mass tends to grow at high density [8]. There has been some attempt to overcome these difficulties by introducing an additional field, the dilaton which is devised to effectively incorporate the trace anomaly in QCD [9]. However, it was shown that a chirally restored phase in the presence of vector-meson coupling to the dilaton is only possible at unphysically high values of compressibility ( $K \geq 1400$  MeV) [9]. This paper is an attempt to resolve both problems, namely high compressibility and the absence of abnormal phase. We will show that inclusion of the

---

<sup>1</sup> Note that assignment of a single meson serving in both roles does not necessarily lead to a consistent picture. For example, in the successful non-chiral Walecka model [4, 5], the scalar meson only plays the role of the mediator of mid-range attraction between nucleons. One should also note that the chiral symmetry realization of the linear sigma model is neither unique nor essential. For example, in a non-linear realization [6], the pions field appears alone and in vector manifestation scenario of Harada and Yamawaki [7], the rho meson is taken as chiral partner of the pions.

Dirac-sea in a non-renormalizable fashion reduces the compressibility. The chiral phase transition is expected to occur at high density where the baryonic degrees of freedom are no longer appropriate. We show that the chiral restoration can be described by incorporating the quark degrees of freedom into the  $L\sigma N$  model at high density. We simulate the quark deconfinement at finite density by changing the active degrees of freedom from nucleons to quarks at high density. This leads to a first order deconfinement phase transition, in accordance with indications from earlier studies [10]. In our simple model quark deconfinement and chiral restoration are interconnected. A general outcome of our analysis concerns the crucial importance of deconfinement for understanding the chiral restoration at finite density.

Initially, the quantum hydrodynamical model was based on renormalizable field theory. Therefore, a systematic inclusion of vacuum loops was necessary in order to accommodate the response of a filled Dirac-sea to the presence of valence nucleons. By renormalizability requirement one could then absorb the vacuum loops and redefine the coefficients of the effective potential. However it was shown that the resulting effective potential does not provide an acceptable description of the properties of finite nuclei, and inclusion of next-to-leading order loop expansion even worsens the situation [11]. Furnstahl *et. al.* [12] showed also that one-baryon-loop vacuum contribution in renormalized models like the  $L\sigma N$  model and the Walecka model give rise to large *unnatural* coefficients based on “naive dimensional analysis” proposed by Georgi and Manohar [14], indicating that the quantum vacuum is not described adequately by long-range degree of freedoms.

One possible resolution to the *unnaturalness* has been non-renormalizable effective field theory approach, where one includes all possible terms consistent with the underlying symmetry, hoping that short-range physics can be taken into account by non-linear higher order interaction terms. In this way, there is no reference to a Dirac sea of nucleons. In this paper, we take a radical approach and introduce an ultraviolet cutoff  $\Lambda$  into the definition of the chiral sigma model. In our approach the cutoff is taken as new extra parameter which needs to be fixed by some phenomenological input. Therefore, our model by default becomes non-renormalizable, similar to the Nambu-Jona-Lasinio (NJL) model [15]. In this way by construction one does not need to absorb the vacuum loops into interaction terms, and therefore the unnaturalness problem can be avoided. With the cutoff we can discard the short-range physics which cannot be described by long-range degrees of freedom. In other words, the sharp cutoff  $\Lambda$  separates the active negative energy states from the ones that does not contribute. In this way, we explicitly retain the intuitive concept of Dirac sea as a counterpart of Fermi sea.

In the first part of the paper (section II) we study nuclear matter properties within an extended

L $\sigma$ N model in present of explicit Dirac-sea. In the second part of paper (section III), we incorporate the quark degrees of freedom above deconfinement density. Having calibrated the parameters of the model to the empirical nuclear matter saturation, we investigate the implication of quark deconfinement in the equation of state and in the description of the chiral restoration. Some concluding remarks are given in section IV.

## II. NUCLEAR MATTER AND NATURALNESS

We consider the chiral L $\sigma$ N model with exact global  $SU(2) \times SU(2)$  symmetry, which contains a pseudoscalar coupling between pions and nucleons, plus an auxiliary scalar field  $\sigma$ . We also include a massive isoscalar vector field  $\omega^\mu$ ,

$$\mathcal{L}_n = \bar{\psi}_n [\gamma_\mu (i\partial^\mu - g_{v n} \omega^\mu) - g_{s n} (\sigma + i\gamma_5 \vec{\tau} \vec{\pi})] \psi_n + \mathcal{L}_{\sigma\pi} + \mathcal{L}_{\sigma\omega}, \quad (1)$$

where  $\mathcal{L}_{\sigma\pi}$  and  $\mathcal{L}_{\sigma\omega}$  are defined as

$$\begin{aligned} \mathcal{L}_{\sigma\pi} &= \frac{1}{2} (\partial_\mu \sigma \partial^\mu \sigma + \partial_\mu \vec{\pi} \partial^\mu \vec{\pi}) + \frac{m_s^2}{2} (\sigma^2 + \vec{\pi}^2) + \frac{\lambda}{4} (\sigma^2 + \vec{\pi}^2)^2, \\ \mathcal{L}_{\sigma\omega} &= -\frac{1}{4} F_{\mu\nu} F^{\mu\nu} + \frac{1}{2} g_v^2 \omega^\mu \omega_\mu (\sigma^2 + \vec{\pi}^2), \end{aligned} \quad (2)$$

and the field tensor is defined  $F_{\mu\nu} = \partial_\mu \omega_\nu - \partial_\nu \omega_\mu$ . The nucleon mass  $M_N$  and vector-meson mass  $m_v$  at rest are generated through spontaneous symmetry breaking by  $\sigma$ -field

$$M_N(\sigma) = g_{s n} \sigma, \quad m_v(\sigma) = g_v \sigma. \quad (3)$$

For uniform nuclear matter, the ground state is obtained by filling energy level with spin-isospin degeneracy  $\gamma_n = 4$  up to the Fermi momentum  $k_F$ , where  $k_F$  is related to the baryon density  $\rho$  by

$$\rho = \frac{\gamma_n}{(2\pi)^3} \int_0^{k_F} d^3k. \quad (4)$$

We employ the conventional mean-field approximation by expanding the meson fields around their expectation values  $\bar{\sigma} = \langle \sigma \rangle$  and  $\bar{\omega}^0 = \langle \omega^0 \rangle$  neglecting meson fluctuations. The mean values of the pion field and space component of the vector field vanish for a baryonic matter at rest due to symmetry. Having used the equation of motion for the  $\bar{\omega}^0$  field, the energy density can be expressed as

$$\begin{aligned} \Omega &= \frac{g_{v n}^2 \rho^2}{2m_v^2(\bar{\sigma})} + \frac{m_s^2}{2} (\bar{\sigma}^2 - \bar{\sigma}_0^2) + \frac{\lambda}{4} (\bar{\sigma}^4 - \bar{\sigma}_0^4) + \gamma_n \int_0^{k_F} \frac{d^3k}{(2\pi)^3} \sqrt{k^2 + M_N^2(\bar{\sigma})} \\ &\quad - \gamma_n \int_0^\Lambda \frac{d^3k}{(2\pi)^3} \left( \sqrt{k^2 + M_N^2(\bar{\sigma})} - \sqrt{k^2 + M_N^2(\bar{\sigma}_0)} \right), \end{aligned} \quad (5)$$

where nucleon and vector masses are defined in Eq. (3). The  $\bar{\sigma}_0$  denotes the mean-value of sigma field in vacuum. The second line in Eq. (5) describes the negative-energy nucleon Dirac-sea contribution  $\Omega_{vac}$  subtracted from its corresponding value at zero density. This term is divergent, we regularize it by a sharp ultraviolet cutoff  $\Lambda$ . The linear sigma model is renormalizable, therefore any cutoff dependence should be removed by some kind of renormalization scheme in a such way that the chiral symmetry of the model is preserved. The vacuum expression can be expanded in powers of  $M_N/\Lambda$  which creates an infinite series in terms of scalar mean-field (notice that the only first four orders are divergent). By employing a renormalization scheme, one can then partly absorb these terms into the coefficients of the effective potential [16] (note also that this procedure is not unique),

$$\Omega_{vac} \simeq -\frac{\gamma_n}{(4\pi)^2} \left( M_N^4 \ln \frac{M_N}{\mu} + \sum_{i=0}^4 a_i (g_{sn} \sigma)^i \right), \quad (6)$$

where  $\mu$  denotes the renormalization scale (which is normally chosen to be nucleon mass at zero density) and  $a_i$  denotes the counterterms. The logarithmic term  $M_N^4 \ln \frac{M_N}{\mu}$ , however cannot be removed in this fashion. The renormalizability requirement imposes very restrictive conditions on these highly nonlinear terms. It has been shown that such a renormalized theory is in apparent conflict with the *naturalness* property based on Georgi's naive dimensional analysis [14]. This indicates that the power counting will not be correct<sup>2</sup>.

The basic assumption of *naturalness* is that once the appropriate dimensional scale has been extracted using “naive dimensional analysis” proposed by Georgi and Manohar [14], the remaining dimensionless coefficients should all remain of order unity. If the naturalness assumption is valid, then the effective Lagrangian can be truncated within a reasonable error. Notice that there is no general proof of the naturalness property, since we do not know how to derive effective hadronic Lagrangian from QCD. Nevertheless, phenomenological studies support the validity of naturalness and naive power counting rules.

The first attempt to make this model compatible with the naturalness property has been to relax the renormalizability requirement and include all non-linear terms which are allowed according to the underlying symmetry [12]. Then, one can fix the parameters of the model with some phenomenological input. In this fashion, no reference to Dirac-sea is invoked and one retains only the valence nucleon explicitly. All vacuum-loop effects will then be hidden in the new interaction

---

<sup>2</sup> Moreover, the resulting renormalized effective model fails to reproduce observed properties of finite nuclei, such as spin-orbit splitting, shell structures, charge densities, etc [13].

terms added to the original model. Here, we follow the same line of idea, namely relaxing the renormalizability condition by adding the ultraviolet cutoff  $\Lambda$  to our model definition, but we keep the concept of the Dirac-sea in a similar way to the non-renormalizable NJL model [15]. Here, the Dirac-sea is explicitly kept without invoking any new ad hoc interaction terms by expansion.

The in-medium scalar mean-field  $\bar{\sigma}$  (and its corresponding value in vacuum  $\bar{\sigma}_0$ ) or equivalently, the effective nucleon mass  $M_N(\bar{\sigma})$  ( and  $M_N(\bar{\sigma}_0)$  at zero density) is determined via the self-consistency condition by minimizing the energy-density  $\Omega(\bar{\sigma})$  with respect to  $\bar{\sigma}$ ,

$$-\frac{4g_{vn}^2 k_F^6}{9\pi^4 g_v^2 \bar{\sigma}^3} + m_s^2 \bar{\sigma} + \lambda \bar{\sigma}^3 + \frac{g_{sn}^2 \bar{\sigma}}{\pi^2} \left[ k_F E(k_F) - \Lambda E(\Lambda) + g_{sn}^2 \bar{\sigma}^2 \ln \frac{\Lambda + E(\Lambda)}{k_F + E(k_F)} \right] = 0, \quad (7)$$

where  $E(k_F)$  and  $E(\Lambda)$  in the above expression are defined by  $E(k) = \sqrt{k^2 + g_{sn} \bar{\sigma}^2}$ . This non-linear equation should be solved for every point of density associated with Fermi-momentum  $k_F$ . The sigma mass is given by

$$m_\sigma^2 = \frac{\partial^2 \Omega}{\partial \bar{\sigma}^2} \quad (8)$$

where the derivatives are evaluated at the scalar mean-field  $\bar{\sigma}$  solution of the gap equation (7). In the presence of the nucleon Dirac-sea, one does not need to constraint the form of potential from outset with  $m_s^2 < 0$  in order to ensure the spontaneous symmetry breaking. The negative energy Dirac-sea contribution can indeed generate a dynamical broken vacuum analogous to the NJL model. Due to spontaneous symmetry breaking the scalar mean field acquires a nonzero vacuum expectation value which is equal to the pion decay constant  $f_\pi$ . Here, the pions are the massless Nambu-Goldstone bosons.

Our model contains six parameters  $g_{sn}, g_v, m_s^2, \lambda, \Lambda$  and  $g_{vn}$ . In contrast to NJL type models, here everything can be determined from the gap equation<sup>3</sup> (7). In the NJL model the meson masses and pion decay should be solved as well since they are described as collective quark-antiquark excitations, while in  $L\sigma N$  model they are represented as dynamical fields. We take the empirical values for pion decay  $f_\pi = 93$  MeV, nucleon mass in vacuum  $M_N(\bar{\sigma}_0) = 939$  MeV and vector-meson mass in vacuum  $m_v(\bar{\sigma}_0) = 783$  MeV. These choices fix  $g_{sn} = M_N/f_\pi = 10.1$  and  $g_v = m_v/f_\pi = 8.42$  via<sup>4</sup> Eq. (3). The vector field coupling  $g_{vn}$  is treated as a free parameter and will be adjusted in medium in such a way that the equation of state reproduces nuclear-matter saturation properties, which we define as a binding energy per nucleon  $E/A = -15.75$  MeV at a density corresponding to

<sup>3</sup> Notice that in general the gap equation may have many solutions, one has to find out which solution minimizes the effective potential.

<sup>4</sup> The value of  $g_{sn}$  differs from the experimental value  $g_{sn} = 13.5$ . This is a typical situation in chiral models with  $g_A = 1$  where nucleons are taken structureless.

TABLE I: The parameters  $\Lambda$ ,  $m_s^2$ ,  $\lambda$  and  $g_{vn}$  for sets  $A1$ ,  $A2$  and  $B1 - B3$  are given (see the text for details). All parameter sets reproduce the empirical saturation point ( $E_B/A = -15.75$  MeV,  $\rho_0 = 0.148$  fm $^{-3}$ ). The corresponding sigma mass  $m_\sigma$  in the vacuum and the resulting nucleon mass  $M_N(\bar{\sigma})|_{\rho_0} = M_N^*$  and the compressibility  $K$  at saturation density are also given.

Parameter	set $A1$	set $A2$	set $B1$	set $B2$	set $B3$
$\Lambda$ (MeV)	256	300	324	444.2	483.2
$m_s^2$ (GeV $^2$ )	-0.147	-0.041	0.026	0.544	0.77
$\lambda$	31.5	27.4	25	7.0	0
$g_{vn}$	6.69	6.62	6.54	6.23	6.07
$m_\sigma(\bar{\sigma}_0)$ (MeV)	806.5	805	810.5	810	817
$M_N^*$ (MeV)	757.2	761.2	766.3	781.3	784.5
$K$ (MeV)	490	478	455	396	370

a Fermi momentum of  $k_F = 1.3$  fm $^{-1}$ . The coupling  $m_s^2, \lambda$  and  $\Lambda$  can be determined by requiring the value of the pion decay  $f_\pi = 93$  MeV and value of sigma meson mass defined in Eq. (8). In this way, one still cannot uniquely fix the value of the cutoff. Therefore, for sake of generality we consider various parameter sets  $A1, A2$  and  $B1 - B3$  given in table I which are determined with the above-mentioned procedure and all pass through the empirical nuclear matter saturation point ( $E_B/A = -15.75$  MeV,  $\rho_0 = 0.148$  fm $^{-3}$ ). The empirical compression modulus (or pressure) is not used in the fitting procedure. Generally, increasing the cutoff shift the saturation point to higher density, however for not very high cutoff (given in table I) one can adjust other parameters in order to reproduce the empirical saturation point. Parameter sets  $A1$  and  $A2$  are chosen with condition that  $m_s^2 < 0$ , (i.e. with initial Mexican hat potential even without inclusion of the Dirac-sea) while for parameter sets  $B1-B3$  we have  $m_s^2 > 0$  (in this case, the Dirac-sea generates a Mexican hat potential). For various parameter sets a sigma-meson of mass about 810 MeV is needed in order to reproduce the empirical saturation point (see table 1). The value of nucleon masses  $M_N^*$  at the saturation point for various parameter sets are also given in table I.

On the right panel of Fig. 1, we show the mean-value of scalar field  $\bar{\sigma}$  with respect to density  $\rho/\rho_0$ . As it is observed as the density is increased the mean-value of scalar field decreases. However, at high density above  $2\rho_0$  the curves (for different parameter sets) bend upward, indicating that the chiral restoration can not be described in this model [8, 9]. This is due to the fact that the model is inadequate in short-distance physics while the meson degrees of freedom  $\sigma$  and  $\omega$  account for nuclear interaction at short distance. Moreover, the vector-meson mass appears in the denominator of the

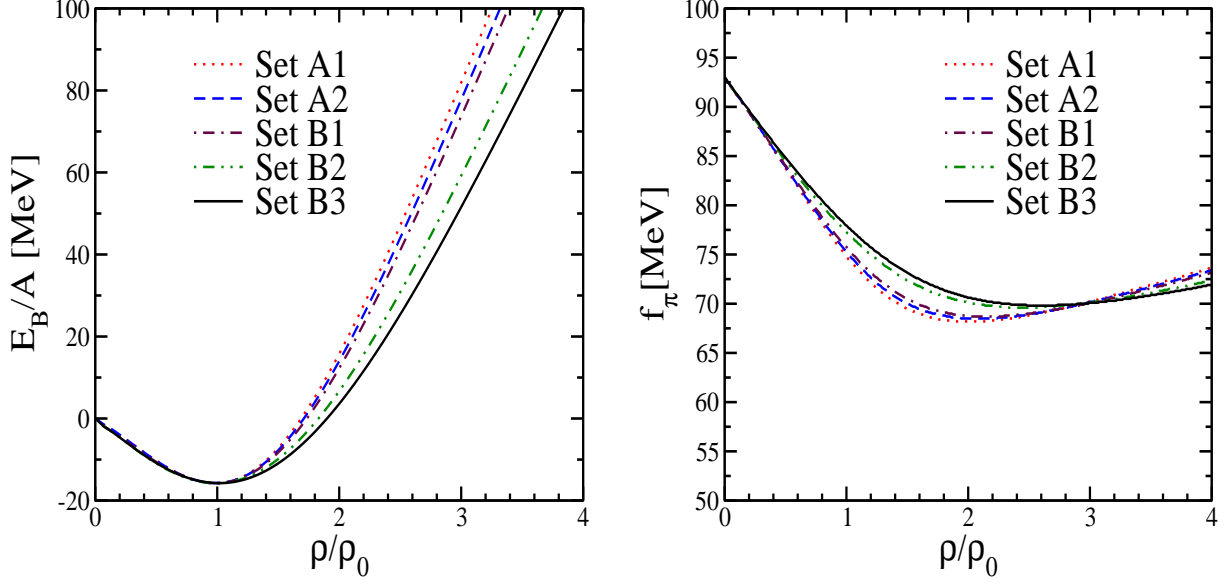


FIG. 1: On the right panel, we show in-medium pion decay as function of density  $\rho/\rho_0$  (with nuclear matter density  $\rho_0 = 0.15 fm^{-3}$ ) for various parameter sets given in table I. On the left panel, we show the binding energy per baryon  $E_B/A$  as a function of density  $\rho/\rho_0$ .

energy density Eq. (5) and cannot vanish. On the other hand, the vector-meson mass is locked to the scalar field by chiral symmetry. Therefore,  $\bar{\sigma}$  as well cannot vanish, our numerical results reflect this fact. In the next section, we will introduce a scenario in which the chiral restoration problem can be resolved.

In Fig. 1 left panel, we show the density dependence of the energy per baryon  $E_B/A = \Omega/\rho - M_N(\bar{\sigma}_0)$  calculated for different parameter sets given in table I. The value of  $\Omega$  is calculated from Eq. (5) by making use of the self-consistency equation (7). It is observed from Fig. 1 that as we increase the cutoff (increasing the contribution of the Dirac-sea) the equation of state becomes softer. In order to find out quantitatively the stiffness of the equation of state, we compute the compression modulus. It is defined as

$$K = 9 \frac{d^2 \Omega}{d\rho^2}. \quad (9)$$

The compression modulus at the saturation density for parameter set B3 and A1 are 370 MeV and 490 MeV, respectively. The compression modulus of other parameter sets lie between these two values (see table I). These values are still bigger than the empirical one  $K = 200 - 300$  MeV [17]. Nevertheless, it improves compared to no-sea approximation where we have  $K \simeq 650$  MeV [8]. Note that it has been shown by Prakash and Ainsworth [18] that the empirical compressibility



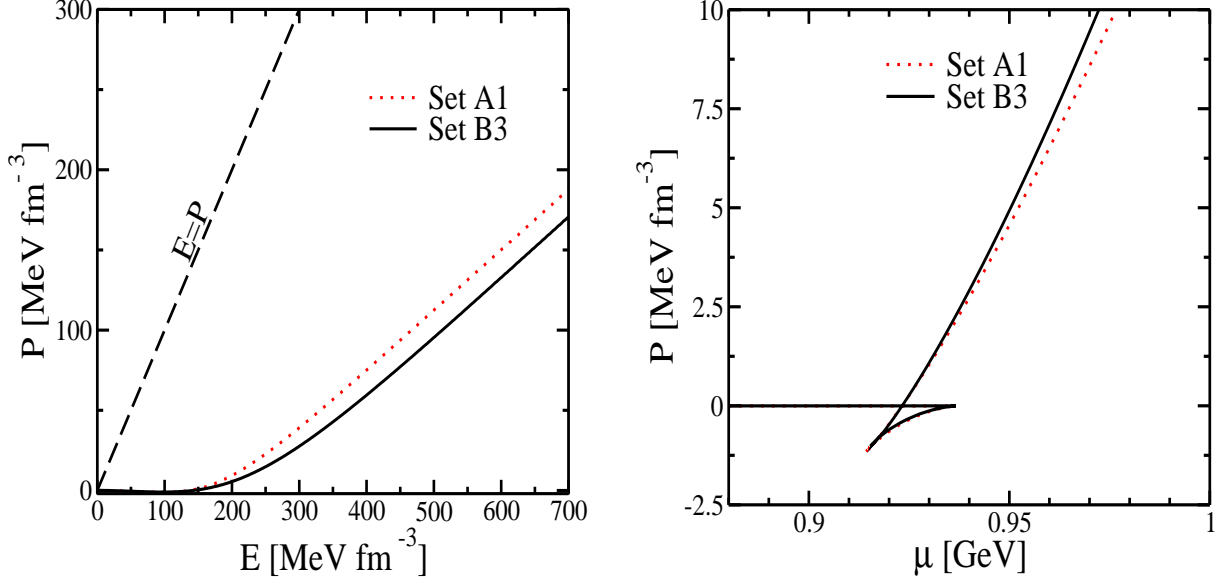


FIG. 2: On the left, the pressure with respect to the energy is shown for parameter sets A1 and B3 given in table I. On the right side, we show the pressure as a function of chemical potential  $\mu$  for the same parameter sets.

can be obtained when the vacuum-loops in a renormalizable fashion are included. However, this results to unacceptably large scalar sigma mass of about 1 GeV and unnaturalsness of the effective Lagrangian as we already discussed. It has been pointed out by Furnstahl and Serot [13] that the scalar meson mass must be light enough in order to avoid strong fluctuations in the charge density, which signal impending instabilities.

By increasing the cutoff, the value of the nucleon mass at saturation density slightly increases. For the various parameter sets given in table I, at saturation we have  $M_N^*/M_N(\bar{\sigma}_0) = 0.81 - 0.84$  which is in good agreement with analysis by Mahaux and Sartor [19].

Next we compute the pressure  $P$  at zero temperature as function of density  $\rho$ , the baryonic chemical potential  $\mu$  and energy. We use thermodynamical identities

$$\mu = \frac{d\Omega}{d\rho}, \quad P = \mu\rho - \Omega = \rho^2 \frac{d}{d\rho} \left( \frac{\Omega}{\rho} \right). \quad (10)$$

In Fig. 2 left panel, we show the pressure  $P$  as function of energy  $E = \Omega$  for set A1 and B3 (other parameter sets behave similarly). The causal limit  $E = P$  is also shown in the figure. It is obvious that all the parameter sets studied here respect the causal condition  $\partial P / \partial E \leq 0$ . Therefore, non-renormalizability in our model does not lead to conflicts with causality. The pressure at vacuum and saturation density is zero  $P(\rho_0) = 0$  which gives a nontrivial constraint on the model parameters. The phase transition becomes more apparent by computing pressure as a function of chemical

potential  $\mu$ . A first order phase transition is manifested by appearance of several branches of  $P(\mu)$ . In Fig. 2 right panel, the pressure with respect to chemical potential for parameter sets *A1* and *B3* are shown. These curves show the liquid-gas phase transition in nuclear matter. The first order phase transition occurs at  $\mu_c \simeq M_N(\bar{\sigma}_0) - 15.75 \simeq 923.25$  MeV for all various parameter sets given in table I. At this point, the slope of curves  $P(\mu)$  exhibits a jump corresponding to difference of densities between coexisting phases. At a fixed chemical potential only the highest pressure corresponds to a stable phase.

Some remarks here are in order. One can observe that as we increase the cutoff, i.e increasing the negative energy Dirac-sea contribution, a stronger coupling  $m_s^2$  (with positive sign) is needed, while the coupling  $\lambda$  substantially decreases (see table I). This can be understood since the Dirac-sea contains many-body forces and in principle there is no need to add arbitrary extra many-body forces in terms of potential into system when the Dirac-sea is enhanced. On the other hand, the nuclear matter saturation properties can be better described (compressibility is reduced) with increasing cutoff in a acceptable range. The Dirac-sea also generates a vacuum with dynamically broken symmetry. Note that the exact connection between the chiral dynamics and nuclear matter saturation mechanism is not yet completely understood. Recently we have shown in a relativistic Faddeev approach [20] that nuclear matter saturation might be related to partial chiral restoration [21].

In the bosonized version of the NJL model,  $\sigma^4$  self-interaction term is absent  $\lambda = 0$  (even in vacuum), therefore our cutoff  $L\sigma N$  model calibrated to nuclear matter saturation properties becomes very similar to the NJL model since we have  $\lambda \rightarrow 0$  as we increase the cutoff (see table I). It is interesting to note as well that in mean field approximation, the nuclear matter in the NJL model does not saturate without inclusion of a vector-scalar fermion self-interaction [22]. Therefore the same saturation mechanism is behind both models. Finally, as can be noticed from table I, the acceptable range of cutoff is too low  $\Lambda \simeq 250 - 485$  MeV. A similar range for the cutoff has been also reported in the NJL model with nucleonic degrees of freedom [22, 23]. This is in contrast with the case that the model is defined in terms of quarks where the allowed range of the cutoff is typically larger. This may indicate that by changing the relevant degrees of freedom from nucleons to quarks, the model can be extended to higher energy.

### III. CHIRAL RESTORATION AND DECONFINEMENT

In this section we consider the implication of quark deconfinement in the nuclear matter equation of state. We incorporate the deconfinement effect by adding the quark dynamics to the nucleonic Lagrangian  $\mathcal{L}_n$  defined in Eq. (1) and assume that at a critical Fermi momentum  $k_C$  (corresponding to a critical density  $\rho_C$ ), the baryonic degrees of freedom are replaced by quark ones, while, keeping the description of scalar and pion fields intact at higher density. We cannot derive the exact value of deconfinement density  $\rho_C$  in the context of mean field theory where the internal structure of hadron is neglected, therefore we do not constrain ourself to only one value for  $\rho_C$  and consider the implication of different values for  $\rho_C$ . The energy density can be written

$$\Omega = \Omega_n + \Omega_q \theta(\rho - \rho_C), \quad (11)$$

where  $\Omega_n$  is obtained from  $\mathcal{L}_n$  defined in Eq. (1) and  $\Omega_q$  is obtained from the following quark Lagrangian

$$\mathcal{L}_q = \bar{\psi}_q [\gamma_\mu i \partial^\mu - g_{sq} (\sigma + i \gamma_5 \vec{\tau} \vec{\pi})] \psi_q + \mathcal{L}_{\sigma\pi} + \mathcal{L}_{\sigma\omega}, \quad (12)$$

where  $\mathcal{L}_{\sigma\pi}$  and  $\mathcal{L}_{\sigma\omega}$  are defined in Eq. (2). We do not couple the vector-meson field directly to the quark field since the vector-meson in this model works against chiral restoration phase transition at high density. Therefore, we assume that the quark field is only coupled to the scalar  $\sigma$  and the pion  $\vec{\pi}$  fields in chirally invariant way. But we allow the vector-meson field to couple to the scalar field through interaction term  $\mathcal{L}_{\sigma\omega}$ . Since quarks are coupled to scalar field, the vector field is not completely decoupled from quarks. The quark mass like the nucleon and vector meson masses Eq. (3) are generated through spontaneous symmetry breaking via scalar field,

$$m_q(\sigma) = g_{sq} \sigma. \quad (13)$$

The energy density  $\Omega$  at finite density in mean field approximation as a function of Fermi momentum can be obtained as

$$\begin{aligned} \Omega = & \frac{2g_{vn}^2}{9\pi^4 m_v^2(\bar{\sigma})} (k_F^6 \theta(k_C - k_F) + \mathcal{R} k_C^6 \theta(k_F - k_C)) + \frac{m_s^2}{2} (\bar{\sigma}^2 - \bar{\sigma}_0^2) + \frac{\lambda}{4} (\bar{\sigma}^4 - \bar{\sigma}_0^4) \\ & + \gamma_n \int_0^{k_F} \frac{d^3 k}{(2\pi)^3} \sqrt{k^2 + M_N^2(\bar{\sigma})} \theta(k_C - k_F) + \gamma_n \int_0^{k_C} \frac{d^3 k}{(2\pi)^3} \sqrt{k^2 + M_N^2(\bar{\sigma})} \theta(k_F - k_C) \\ & + \gamma_q \int_{k_C}^{k_F} \frac{d^3 k}{(2\pi)^3} \sqrt{k^2 + m_q^2(\bar{\sigma})} \theta(k_F - k_C) - \gamma_n \int_0^{k_C} \frac{d^3 k}{(2\pi)^3} \left( \sqrt{k^2 + M_N^2(\bar{\sigma})} - \sqrt{k^2 + M_N^2(\bar{\sigma}_0)} \right) \\ & - \gamma_q \int_{k_C}^{\Lambda} \frac{d^3 k}{(2\pi)^3} \left( \sqrt{k^2 + m_q^2(\bar{\sigma})} - \sqrt{k^2 + m_q^2(\bar{\sigma}_0)} \right), \end{aligned} \quad (14)$$

where the quark mass  $m_q$ , the nucleon mass  $M_N$  and the vector-meson mass  $m_v$  are defined in Eqs. (3,13).  $\gamma_q = 12$  and  $\gamma_n = 4$  are the degeneracy factor for quarks and nucleon, respectively. We have also included the corresponding Dirac-sea of the nucleons and the quarks as in the previous section. A priori we do not know the importance of the vector-scalar interaction above deconfinement density. We consider two cases above the critical deconfinement density  $\rho_C$ :  $g_v = 0$  corresponding to totally decoupling of the vector field from matter and  $g_v \neq 0$  when the vector-scalar interaction is present<sup>5</sup>. In the energy density equation (14), the parameter  $\mathcal{R}$  can have two values  $\mathcal{R} = 0, 1$  corresponding to the solutions when  $g_v = 0$  and  $g_v \neq 0$  above the critical deconfinement density  $\rho_c$ , respectively. Note that the parameter  $\mathcal{R}$  was merely introduced in order to write both solutions in one equation.

The Fermi momentum  $k_F$  can be related to baryonic density by

$$\rho = \frac{2k_F^3}{3\pi^2}. \quad (15)$$

The mean-value of scalar field  $\bar{\sigma}$  is determined by in-medium gap equation:

$$\begin{aligned} & - \frac{4g_{vn}^2}{9\pi^4 g_v^2 \bar{\sigma}^3} (k_F^6 \theta(k_C - k_F) + \mathcal{R} k_C^6 \theta(k_F - k_C)) + m_s^2 \bar{\sigma} + \lambda \bar{\sigma}^3 + f_q(k_C) - f_q(\Lambda) \\ & - f_n(k_C) + f_n(k_F) \theta(k_C - k_F) + (f_n(k_C) + f_q(k_F) - f_q(k_C)) \theta(k_F - k_C) = 0, \end{aligned} \quad (16)$$

with

$$f_x(k) = \frac{\gamma_x g_{sx}^2 \bar{\sigma}}{4\pi^2} \left( k \sqrt{k^2 + (g_{sx} \bar{\sigma})^2} - (g_{sx} \bar{\sigma})^2 \ln \frac{k + \sqrt{k^2 + (g_{sx} \bar{\sigma})^2}}{(g_{sx} \bar{\sigma})^2} \right), \quad (17)$$

where we used the notation that  $x = q, n$  stands for the quark and the nucleon terms, respectively.

The quark interaction term Eq. (12) introduces a new extra parameter  $g_{sq}$  which is fixed by choosing the quark mass at vacuum  $m_q(\sigma_0) = 300$  MeV, therefore we have  $g_{sq} = 3.23$ . The other parameters are determined for a given value of deconfinement density  $\rho_C$  (or associated Fermi momentum  $k_C$ ) in the same procedure described in section II, so as to reproduce the empirical nuclear matter saturation point ( $E_B/A = -15.75$  MeV,  $\rho_0 = 0.148$  fm<sup>-3</sup>). Therefore, we calibrate all parameters to nuclear matter properties. We choose again,  $M_N(\sigma_0) = 939$  MeV,  $m_v = 783$  MeV and  $f_\pi = 93$  MeV in vacuum. Notice that, here the cutoff  $\Lambda$  depends on the deconfinement density or equivalently Fermi momentum  $k_C$ , see Eq. (14). This is in fact a cutoff available for a quark in the phase space measured relative to the critical deconfinement Fermi momentum  $k_C$ . A density dependent cutoff was also invoked by Harada, Kim and Rho [24] to study the chiral restoration in the context of vector manifestation scenario of Harada and Yamawaki [7].

---

<sup>5</sup> In this case, the value of the coupling  $g_v$  is fixed by the empirical vector-meson mass in vacuum.

TABLE II: The parameters  $\Lambda$ ,  $m_s^2$ ,  $\lambda$  and  $g_{vn}$  are shown for sets  $C1$  and  $C2$  for two values of the critical deconfinement density  $\rho_C$ . We assume a cutoff  $\Lambda = 483.2$  MeV and the coupling  $g_{sq} = 3.226$  (which yields constituent quark mass 300 MeV) for all parameter sets. All parameter sets reproduce the empirical saturation point ( $E_B/A = -15.75$  MeV,  $\rho_0 = 0.148$  fm $^{-3}$ ). The corresponding sigma mass  $m_\sigma$  in the vacuum and the resulting in-medium nucleon mass  $M_N^*$  at saturation density are also given.

Parameter	set $C1$	set $C2$
$k_C$ (MeV)	368.8 ( $\rho_C = 3\rho_0$ )	292.7 ( $\rho_C = 1.5\rho_0$ )
$m_s^2$ (GeV $^2$ )	0.48	0.376
$\lambda$	15	20
$g_{vn}$	6.35	6.54
$m_\sigma(\bar{\sigma}_0)$ (MeV)	815	807
$M_N^*$ (MeV)	772.2	762.3

In contrast to the case that transition to quark degrees of freedom is not incorporated, here the cutoff can be taken larger and cutoff-dependence is less pronounced. In order to compare our result with the previous section we take the cutoff given in table I for set  $B3$ ,  $\Lambda = 483.2$  MeV. In table II, we show two sets of parameters determined for the fixed cutoff  $\Lambda = 483.2$  MeV assuming that deconfinement take place at density  $\rho_C = 3\rho_0$  and  $1.5\rho_0$  for parameter sets  $C1$  and  $C2$ , respectively. As we already pointed out the cutoff depends on the deconfinement density, this means for a fixed cutoff one needs to adjust other parameters in order to reproduce again given phenomenological input, see table II.

In Fig. 3 left panel, we show the mean-value of scalar field as a function of density for various parameter sets  $B3$  and  $C1, C2$  in the presence of the vector-scalar interaction terms  $g_v \neq 0$  given in table II. For comparison, we also plotted again the corresponding result for parameter set  $B3$  given in table I (without the deconfinement effect). It is seen that exactly at the critical deconfinement density  $\rho_C$ , the slope of in-medium scalar-mean field changes toward chiral restoration (for set  $C2$  this is more obvious). This is in contrast to pure nuclear matter case set  $B3$  (see also Fig. 1 left panel) where chiral restoration seems to be in conflict with nuclear matter properties. On the right panel of Fig. 3, we show the binding energy per baryon for various sets. It is seen that the equation of state at very high density  $\rho \approx 9\rho_0$  become softer than pure nuclear matter. At the deconfinement density there is a pronounced kink which is more obvious if the deconfinement occurs at lower density (see Fig. 3, set  $C2$ ). This is due to the fact that a sharp boundary is assumed between the baryonic and the quark phases. In principle, instead of the theta function in

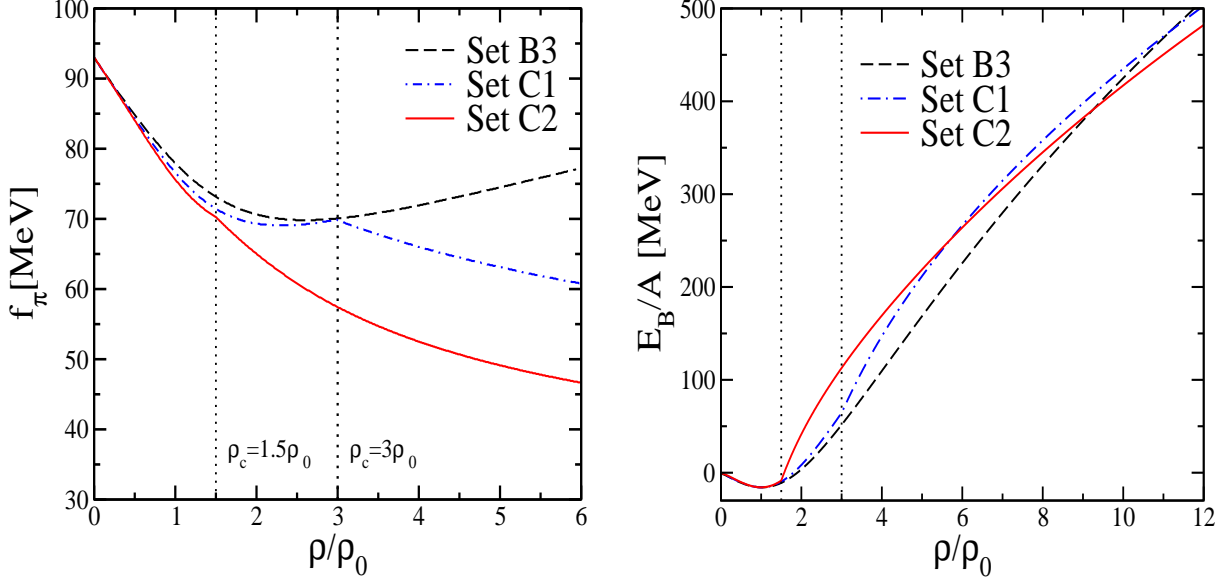


FIG. 3: On the left panel: the scalar mean-field values with respect to density  $\rho/\rho_0$  (with nuclear matter density  $\rho_0 = 0.15 fm^{-3}$ ) is shown when  $g_v \neq 0$  for various parameter sets *B3* and *C1, C2* given in table I and II, respectively. On the right panel: we show the binding energy per baryon  $E_B/A$  as a function of density  $\rho/\rho_0$  for the same sets of parameters. The vertical dotted lines show the positions of the critical deconfinement density  $\rho_C$ .

Eq. (14) one may employ a smooth function. Note also that here the formation of Cooper pairs and color-superconductivity is not taken into account [10]. It has been shown that such effects might have important consequences for the transition to quark matter within compact stars [25]. In particular, diquark degrees of freedom seem to be essential for the emergence of coexistence region between the hadronic and deconfined phases [26].

Next, we switch off completely the vector-scalar interaction term  $g_v = 0$ , (i.e.  $\mathcal{R} = 0$  in Eq. (14)) above the deconfinement density  $\rho_C$ . In Fig. 5, we show the mean-value of scalar field as a function of density for parameter sets *C1* and *C2* when  $g_v = 0$  for  $\rho > \rho_C$ . If the deconfinement take place at higher density the chiral phase transition will be stronger and coincide with the deconfinement critical density. In this case the chiral phase transition is first order. While for a soon deconfinement (for example, parameter set *C2*) the chiral symmetry is partially restored at the deconfinement density and full chiral restoration postpones at relatively higher density than the deconfinement density  $\rho_C$ . It is interesting to note that the soon deconfinement (parameter set *C1*) is not compatible with Brown-Rho scaling [27],

$$\frac{f_\pi(\sigma)}{f_\pi(\sigma_0)} \approx \frac{M_N(\sigma)}{M_N(\sigma_0)} \approx \frac{m_v(\sigma)}{m_v(\sigma_0)}, \quad (18)$$

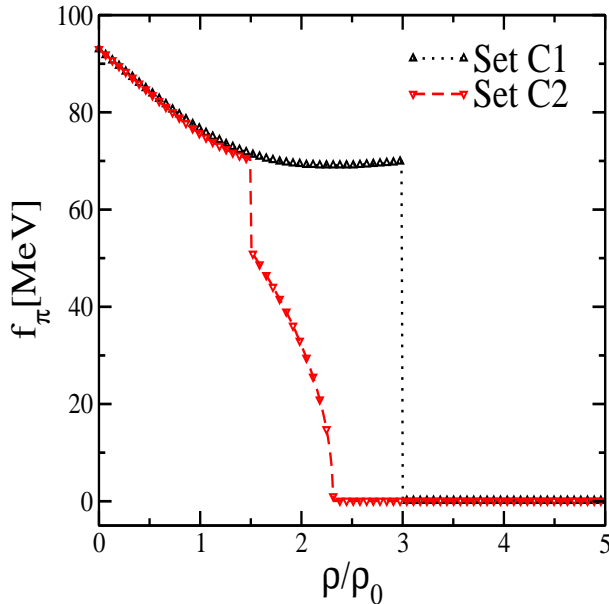


FIG. 4: We show the scalar mean-field values  $f_\pi$  as a function of density  $\rho/\rho_0$  for parameter sets *C1* and *C2* given in table II when the vector-coupling  $g_v$  is zero above the critical deconfinement density  $\rho_C$ .

since we have  $m_v(\sigma) = 0$  above the deconfinement when  $g_v = 0$ , but as it can be seen from Fig. 5 for parameter set *C1*, the mean-value of scalar field  $f_\pi$  above the deconfinement is partially restored and is not zero. If we assume that Brown-Rho scaling is valid at various density, we can put a constraint from below on the onset of critical deconfinement density  $\rho_C$  in our minimal Lagrangian model. We found that for the deconfinement density  $\rho_C \geq 2\rho_0$ , we have  $f_\pi(\rho_C) = 0$  and  $m_v(\rho_C) = 0$  at the same time consistent with Brown-Rho scaling and vector manifestation scenario which is considered to be a generic feature of effective field theory matched to QCD [7]. Therefore, for  $\rho_C \geq 2\rho_0$ , the chiral restoration is first order and coincide with the critical deconfinement density  $\rho_C$ .

#### IV. CONCLUSION

We investigated the implication of the baryonic Dirac-sea in the presence of an explicit ultraviolet cutoff in the nuclear matter equation of state within the  $L\sigma N$  model. In this way, the model becomes non-renormalizable and one can avoid the unnaturalsness problem [12]. We investigated the parameter space of the model as a function of cutoff which reproduces the empirical nuclear matter properties. Note that the empirical compression modulus was not used in the fitting procedure. We showed that a filled Dirac sea of baryons can produce a strong attraction in nuclear matter. It

softens the equation of state and it generates a vacuum with dynamically broken symmetry even without a presence of a negative mass term in the linear sigma model. This also clarified a possible connection between the chiral  $L\sigma N$  model and bosonized version of the NJL model in a nuclear matter medium.

Although the  $L\sigma N$  model in the presence of the vector-scalar interaction can describe the nuclear matter saturation, it is unable to accommodate the chiral restoration phase transition with  $f_\pi = 0$ . The role of vector-meson is very subtle in this model. On one hand it is needed in order to reproduce the empirical saturation properties, but it works against the chiral restoration at high density. In order to study the implication of the first-order deconfinement effect in the equation of state and chiral phase transition, we simulated the deconfinement effect by changing the active degrees of freedom from nucleons to quarks above the critical deconfinement density. At the moment, we do not know yet the order of a possible deconfinement transition and its critical density. However, there are some indications that it might be first order and takes place at about several times the nuclear matter density [10]. Here, we considered the implication of different choices of the critical deconfinement density. We investigated the role of the vector-meson and the deconfinement effect in describing the chiral phase transition when our model parameters are calibrated to the nuclear matter properties. The nature of the chiral phase transition is sensitively dependent on the presence of the vector-scalar interaction. The vector-meson has been reported by many authors to be important for realization of the chiral phase transition [28]. We showed that if the vector-meson is completely decoupled from the quark matter  $g_v = 0$  above the critical deconfinement density, chiral phase transition can take place and its position depends on the given critical deconfinement density. We showed in order to be consistent with Brown-Rho scaling [27] and vector-realization [7] based on hidden-local symmetry, the critical deconfinement density must be bigger than  $2\rho_0$  where  $\rho_0$  is the nuclear matter density. Then the chiral restoration is first order and is coincident with the deconfinement density<sup>6</sup>.

It is of interest to extend scheme presented in this paper to finite temperature and also study the implication of this nuclear-quark equation of state on neutron star.

---

<sup>6</sup> Notice that in contrast with the finite density where Lattice simulation is plagued with sign problem, lattice calculation has been very fruitful for finite-temperature (at zero baryon density) studies [29]. An analysis of the lattice simulation shows that chiral symmetry restoration and deconfinement phase transition occurs at the same temperature [29, 30]. It has been also shown that the vector coupling is small compared to the scalar coupling at high temperature [31].



### Acknowledgements

The author is very grateful to Hans J. Pirner for very fruitful discussions and to Jörg Raufeisen for careful reading of the manuscript and comments. This work was supported by the Alexander von Humboldt foundation.

- 
- [1] See e.g., N. K. Glendenning, *Compact stars*, New York, Springer (1997).
  - [2] B. Müller, nucl-th/0508062 (and references therein).
  - [3] A. K. Kerman and L. D. Miller, Lawrence Berkeley Laboratory Report No. LBL-3675, (1974).
  - [4] J. D. Walecka, Ann. Phys. (N.Y.) **83**, 491 (1974).
  - [5] B. D. Serot and J. D. Walecka, Int. J. Mod. Phys. **E6**, 515 (1997).
  - [6] S. Weinberg, Phys. Rev. Lett. **18**, 188 (1967).
  - [7] M. Harada and K. Yamawaki, Phys. Rev. Lett. **86**, 757 (2001); Phys. Rep. **381**,1 (2003).
  - [8] J. Boguta, Phys. Lett. **120B**, 34 (1983); **128B**, 19 (1983).
  - [9] P. Papazoglou, J. Schaffner, S. Schramm, D. Zschesche, H. Stocker and W. Greiner, Phys. Rev. **C55**, 1499 (1997).
  - [10] K. Rajagopal and Frank Wilczek, hep-ph/0011333; M. Alford, Ann. Rev. Nucl. Part. Sci. **51**, 131 (2001)(and references therein).
  - [11] R. J. Furnstahl, R. J. Perry and B. D. Serot, Phys. Rev. **C40**, 321 (1989).
  - [12] R. J. Furnstahl, B. D. Serot and H.-B. Tang, Nucl. Phys. **A618**, 446 (1997).
  - [13] R. J. Furnstahl and B. D. Serot, Phys. Rev. **C47**, 2338 (1993).
  - [14] H. Georgi, Ann. Rev. Nucl. Part. Sci. **43**, 209 (1993); A. Manohar and H. Georgi, Nucl. Phys. **B234**, 189 (1984).
  - [15] S. P. Klevansky, Rev. Mod. Phys. **64**, 649 (1992).
  - [16] T. D. Lee and G. C. Wick, Phys. Rev. **D9**, 2291 (1974); T. Matsui, B. D. Serot, Ann. Phys. **144**, 107 (1982).
  - [17] See e.g., P. Danielewicz, R. Lacey and W. G. Lynch, Science **298**, 1592 (2002); J. P. Blaizot, Phys. Rept. **64**, 171 (1980).
  - [18] M. Prakash and T. L. Ainsworth, Phys. Rev. **C36**, 346 (1987).
  - [19] E. Mahaux and R. Sartor, Nucl. Phys. **A475**, 247 (1987).
  - [20] A. H. Rezaeian, hep-ph/0507304 (and references therein); A. H. Rezaeian, N. R. Walet, M. C. Birse, Phys. Rev. **C70**, 065203 (2004).
  - [21] A. H. Rezaeian, H. J. Pirner, Nucl. Phys. **A769**, 35 (2006).
  - [22] V. Koch, T. S. Biro, J. Kunz and U. Mosel, Phys. Lett. **B185**, 1 (1987).
  - [23] T. J. Burvenich and D. G. Madland, Nucl. Phys. **A729**, 769 (2003).

- [24] M. Harada, Y. Kim and M. Rho, Phys. Rev. **D66**, 016003 (2002).
- [25] M. Alford and S. Reddy, Phys. Rev. **D67**, 074024 (2003); M. Baldo, M. Buballa, G.F. Burgio, F. Neumann, M. Oertel and H.-J. Schulze, Phys. Lett. **B562**, 153 (2003).
- [26] A. H. Rezaeian, H. J. Pirner, under preparation.
- [27] G. E. Brown and M. Rho, Phys. Rev. Lett. **66**, 2720 (1991);
- [28] M. Buballa, Phys. Rept. **407** 205 (2005)(and references therein).
- [29] F. Karsch, Lect. Notes Phys. **583**, 209 (2002)[hep-lat/0106019].
- [30] J. Kogut, M. Stone, H. W. Wyld, W. R. Gibbs, J. Shigemitsu, S. H. Shenker, D. K. Sinclair, Phys. Rev. Lett. **50**, 393 (1983); F. Karsch and E. Laermann, Phys. Rev. **D50**, 6954 (1994).
- [31] G. Boyd, S. Gupta, F. Karsch and E. Laermann, Z. Phys. **C64**, 331 (1994).